

MINERALOGICAL MAGAZINE

VOLUME 57 NUMBER 387 JUNE 1993

Mineral chemistry, geothermobarometry and pre-Alpine high-pressure metamorphism of eclogitic amphibolites and mica schists from the Schobergruppe, Austroalpine basement, Eastern Alps

BERNHARD SCHULZ

Institut für Geologie und Mineralogie der Universität Erlangen-Nürnberg, Schloßgarten 5, D-8520 Erlangen, Germany

Abstract

Alternating eclogitic amphibolites, mica schists and orthogneisses in the Schobergruppe to the south of the Tauern Window suffered a post-Upper-Ordovician progressive deformation D_1 – D_2 which produced parallel planar-linear structures in all the rocks. Zoned garnets, preferentially oriented zoned clinopyroxenes (Jd 35–42%) and albite (An 7–9%) give evidence of high-pressure metamorphism (550–650 °C, 14–16 kbar) of the metabasites. Ca-amphiboles crystallized during subsequent decompression. In a kyanite–staurolite–garnet mica schist 300 metres below the metabasites, garnet-bearing assemblages grew synchronous with the development of foliations S_1 and S_2 . Garnets are zoned with increasing X_{Mg} and decreasing–increasing–redecaying X_{Ca} from cores to rims. Albitic plagioclase (An 1–3%) and micas are enclosed in garnet cores and rims, are in contact with garnet, and occur with garnet in microlithons. When these minerals are used for geothermobarometry, a prograde P – T evolution (460 to 680 °C) with coeval pressure variations which reach high-pressure conditions can be estimated. This suggests that garnet–plagioclase geobarometry with albitic plagioclase works in the relevant P – T field. Similar garnet zonation trends and a similarly shaped P – T path from mica schists of an adjacent region with late-Variscan cooling ages, points to an early-Variscan age of the syn- D_1 – D_2 high-pressure and subsequent amphibolite-facies metamorphism.

KEYWORDS: mineral chemistry, garnet–plagioclase barometry, P – T – t -deformation paths, Variscan, Austroalpine basement.

Introduction

PRESSURE–TEMPERATURE–TIME (P – T – t) histories of eclogites in the Austroalpine basement of the Eastern Alps have been the subject of recent research. There is clear evidence of high-pressure metamorphism of eclogites from the type localities Saualpe and Koralpe (Manby and Thiedig, 1988; Miller, 1990), of clinopyroxene–

garnet amphibolites in the Polinik unit of the Kreuzeckgruppe (Hoke, 1990), of eclogites in the Silvretta (Maggetti and Galetti, 1988), and of eclogites of the Ötztal crystalline (Hoinkes *et al.*, 1982; 1991; Mogessi and Purtscheller, 1986). All these Austroalpine eclogites are surrounded and interlayered by paragneisses and mica schists which display amphibolite-facies assemblages of well-established Variscan and/or early-Alpine

overprinting. Thus, a pre-Variscan, especially a Panafrikan and/or 'Caledonian' age of the preceding high-pressure event is thought possible (e.g. Becker *et al.*, 1987; Ebner *et al.*, 1987) for the parts of the basement where early-Alpine reworking is lacking. The present paper describes the metamorphism of metabasites and adjacent kyanite-staurolite-garnet mica schists of the Prijakt area, Schobergruppe, in Eastern Tyrol, Austria. A close relationship between microstructures of early progressive deformation and mineral-chemical evolution allows reconstruction of syn-deformational P - T paths. Garnet-plagioclase geobarometry with garnet and coexisting albitic plagioclase in mica schists, and pressure estimates from the eclogitic amphibolites yield similar results. This gives evidence of a common post-Upper-Ordovician high-pressure metamorphism of both rock types.

Regional geological setting

Several pre-Alpine lithological associations of metamorphic rocks can be distinguished in the Austroalpine basement between the Tauern Window and the Periadriatic Lineament (Fig. 1a, b). A metapsammopelitic unit (MPU) which contains the eclogitic amphibolites at its base, overlies a metapsammopelite-amphibolite-marble unit (AMU) exposed to the north. Orthogneisses with Upper-Ordovician Rb-Sr whole rock isochrons (Borsi *et al.*, 1973; Troll *et al.*, 1976; Hammerschmidt, 1981) and U-Pb zircon ages (Cliff, 1980), interpreted as dating the intrusion of the granitoids, are found in both 'Altkristallin' units. An increasing early-Alpine reworking of the basement to the north is obvious from Variscan-Alpine 'mixing ages', and from Rb-Sr and K-Ar cooling ages (70-90 Ma,

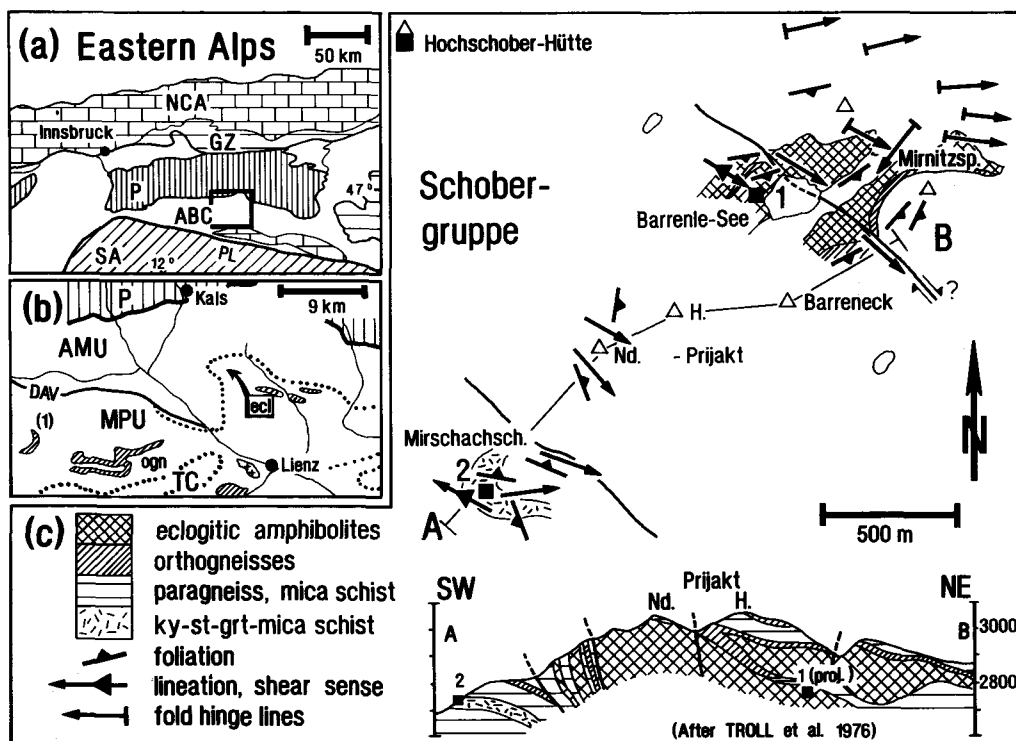


FIG. 1. (a) Geological setting and regional geology in the Eastern Alps. (b) Pre-Alpine units to the south of the Tauern Window. The arrow points to the sampled area in the Schobergruppe. The location of the study by Schulz (1990) in the southern Deferegggen Alps is marked by (1). (c) Structural geology, profile and sampling sites in the Schobergruppe. ABC Austroalpine basement complex; AMU amphibolite-marble unit; DAV Deferegggen-Antholz-Vals-Line (late-Alpine); ecl eclogitic amphibolites in the Schobergruppe area; GZ Grauwackenzone; MPU meta-psammopelitic unit; NCA Northern Calcareous Alps; ogn orthogneisses; P Penninic unit (Tauern Window); PL Periadriatic Lineament; SA Southern Alps; TC Thurmtaler complex.

Oxburgh *et al.*, 1966; Brewer, 1969; Troll, 1978) in the northern part of the MPU and in the AMU (Behrmann, 1990).

In the Prijakt area, Schobergruppe (Fig. 1c), two large bodies of a 700 m thick metabasite sequence occur in the basal part of the MPU and belong to the 'Hangendkomplex' referred to by Clar (1927) and Troll and Hölzl (1974). Strongly foliated orthogneisses partly exceeding 10 m thickness, paragneisses and mica schists concordantly overlie, underlie and are intercalated with the metabasites. The metabasites are MORB tholeiites, the flat *REE* patterns are slightly enriched in *LREE*, and Ce_N/Yb_N ranges from 1.4 to 3.2 (Schulz *et al.*, 1993). Lithological changes with heterogeneously banded cm- to dm-thick layers of eclogitic amphibolites, garnet amphibolites and amphibolites define a planar structural element ('foliation') which is parallel to the gently SE dipping foliation (S_2) of the host rocks. A linear fabric by preferentially oriented amphibole, clinopyroxene and zoisite in metabasites, linear-planar fabrics with elongated quartz-feldspar aggregates, asymmetric augen structures and a flattened S-C geometry in orthogneisses, mineral lineation and foliation in paragneisses, and planar-linear fabrics in mica schists with successive foliations and crenulation lineation are parallel in all the rocks and were produced by an early progressive deformation D_1 - D_2 . A presumably early generation of open to tight folds (B_2 of Troll *et al.*, 1976, 1980) shows fold hinge lines parallel to the SE-plunging lineation. Later folds with NE-SW striking hinge lines deform the lineation and are minor structures of kilometre-scale syn- and antiforms (deformation D_i of Behrmann, 1990) with gently dipping axial planes (Fig. 1c).

No hints to an 'exotic' origin of the metabasites can be derived from their geochemical signatures and the rocks probably represent former basic intrusions into an old continental crust. Furthermore, orthogneiss layers which can be derived from former Upper-Ordovician granitoid intrusions (Troll *et al.*, 1976), occur in a similar manner within metabasites and host rocks and confirm a common history of the sequence since early-Palaeozoic times. A common deformation of the rocks is obvious from the parallel planar and linear structures. However, despite their common lithotectonic history, an apparently different metamorphism is displayed by eclogitic amphibolites with high-pressure garnet-clinopyroxene assemblages (Richter, 1973; Troll *et al.*, 1976) and mica schists bearing amphibolite-facies assemblages which partly formed after the early main deformation (Troll *et al.*, 1976; Behrmann, 1990).

Mineral chemistry in an eclogitic amphibolite (sample 1)

The metabasites are composed of individual layers with varying grain sizes and modes of amphibole, garnet, zoisite, epidote and clinopyroxene (Troll and Hölzl, 1974; Troll *et al.*, 1976). A coarse-grained eclogitic amphibolite (sample 1 from the lower body, see Fig. 1c) shows textural evidence of an eclogitic assemblage of garnet + clinopyroxene + plagioclase + quartz + rutile (Fig. 2a) and a subsequent assemblage of Ca-amphibole + zoisite + plagioclase + quartz + rutile (Fig. 2b, c). Idiomorphic and round garnets enclose quartz, rutile and epidote in their cores; plagioclase and quartz were found in the rims. A zonation of the porphyroblasts with Alm 53-52%, Prp 15-23%, Grs 27-22% and Sps 3-1% from cores to rims (Fig. 2e) suggests a metamorphism slightly prograde in temperature. Many clinopyroxenes are oriented with their long axes parallel to the lineation, but some crystals are oblique to this direction (Fig. 2a-c). Some clinopyroxenes are rimmed by fine-grained symplectites and rarely show breakdown to amphibole and plagioclase (Fig. 2c). Jadeite (Jd) contents of the unchanged omphacites range from 38 to 42 mole %. Analyses from cores yielded Jd 35%, implying slightly increasing jadeite contents towards the rims (Fig. 2d). Plagioclase is found enclosed by garnet rims (Fig. 2a) and as small interstitial xenoblasts together with quartz in the matrix between garnets, clinopyroxenes, amphiboles and zoisites. Other plagioclases seem to be products of a clinopyroxene breakdown reaction (Fig. 2c). Anorthite contents vary slightly from 7 to 9 mole % without relation to the microstructural position of the xenoblasts. Epidotes enclosed in garnet cores have lower Al (4.33, always per formula unit, p.f.u.) and higher Fe (2.11) contents than homogenous long prismatic preferentially oriented zoisites and clinozoisites (Al 5.2, Fe 0.9) in the anisotropic matrix (Table 1b, c). Paragonite (Na 1.6; Mg 0.035; Fe 0.05; Si 6.0) with (001)-planes parallel to the lithological layering displays marginal conversion to biotite.

Thin stripes of green amphiboles with X_{Mg} 0.55 rim some idiomorphic garnets and seem to be products of a garnet-consuming reaction (Fig. 2a). Abundant large optically zoned long-prismatic porphyroblasts (X_{Mg} 0.65-0.75) with pale-green cores and green rims form the mineral lineation (Fig. 2b). Cationic formulae and Fe^{3+} contents of amphiboles were calculated according to Leake (1978) and Papike (1974). They are pargasites, hastingsites and ferri-pargasitic hornblendes which show an evolutionary trend

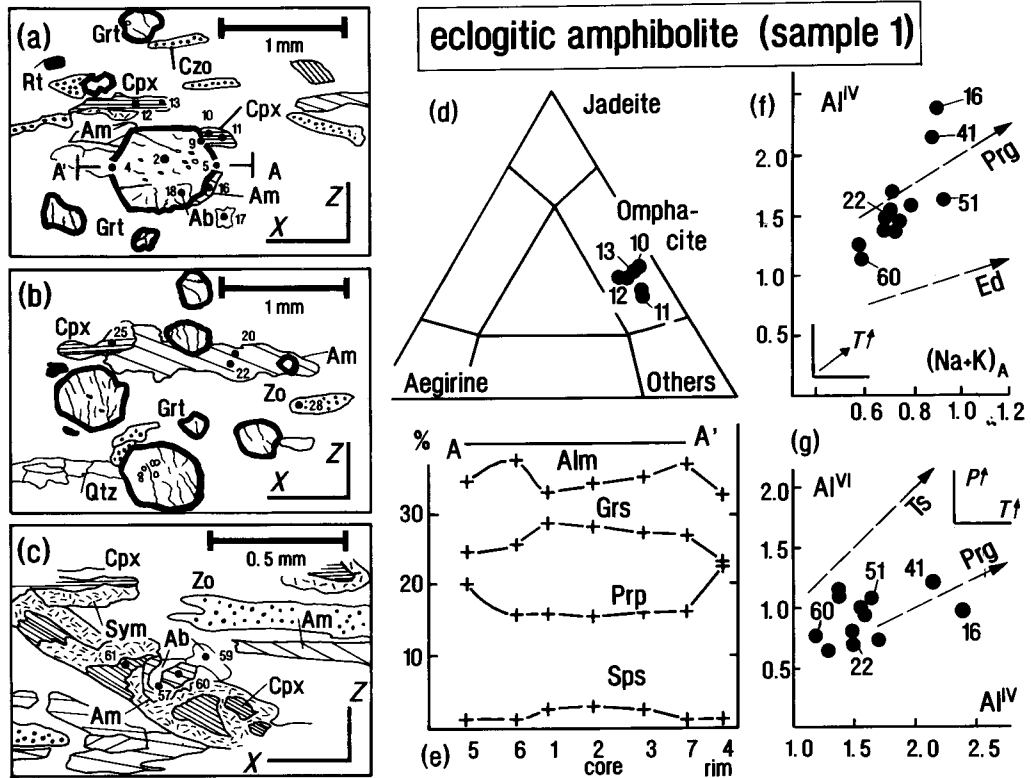


FIG. 2. Microstructures and mineral chemistry in an eclogitic amphibolite (sample 1). Sections parallel to the mineral lineation. Numbers refer to analyses in Table 1 and Fig. 6b. (a) Garnet (Grt, see Fig. 2e for zonation profile) is in contact with preferentially oriented clinopyroxene (Cpx), and is partly rimmed by green amphibole (Am). Garnet encloses albite (Ab). Garnet, clinopyroxene and albite belong to an eclogitic assemblage. (b) Optically zoned amphibole forms mineral lineation (\cong X) and encloses garnet. (c) Fine-grained symplectites (Sym) rimming clinopyroxene, and green amphibole with albite from clinopyroxene breakdown belong to a post-eclogitic assemblage. (d) Compositions of clinopyroxenes in the omphacite field. (e) Zonation profile A-A' of the garnet in Fig. 2a in almandine (Alm), grossular (Grs), pyrope (Prp), and spessartine (Sps) contents. (f) Compositions of amphiboles in Al^{IV} versus $(Na + K)_A$ diagram. (g) Compositions of amphiboles in Al^{VI} versus Al^{IV} diagram.

from high to low $(Na + K)_A$ (1.0 to 0.6) and Al^{IV} (2.4 to 1.2) values at slightly variable Al^{VI} (1.0) contents (Fig. 2f, g). The amphiboles rimming garnet seem to have grown earlier than the porphyroblasts.

P-T estimates from eclogitic amphibolite (sample 1)

Temperature limits are obtained from Fe^{2+} -Mg exchange garnet-clinopyroxene geothermometers. Application of calibrations by Raheim and Green (1974), Ellis and Green (1979) and Krogh (1988) to immediate contact pairs and rim-rim pairs of garnets and clinopyroxenes gives temperatures between 600 and 650 °C at assumed fixed pressures (Fig. 6b). Similar calculations with

garnet and clinopyroxene cores of adjacent porphyroblasts (Fig. 2a) yields lower temperatures from 550 to 600 °C. Pressures were estimated by using the albite-jadeite-quartz geobarometers of Holland (1983) and Gasparik and Lindsley (1980). Jadeite contents of 35 mole % in clinopyroxene cores and up to 42 mole % in the rims lead to pressures around 14 and 15 kbar at 550–650 °C. Pressure estimates from the clinopyroxene-garnet-plagioclase geobarometer of Perkins and Newton (1981), applied to the garnet-clinopyroxene pairs described above and in equilibrium with matrix plagioclase, are 14 kbar at 550–600 °C, and 16 kbar at 600–650 °C. The P-T fields enclosed by minimal and maximal results from all applied calibrations (Fig. 6b), display increasing temperatures from 550 to 650 °C and moderately increas-

TABLE 1. (a)–(c) Microprobe analyses from eclogitic amphibolite (sample 1), selected from 65 analyses. Numbers of oxygens: garnet 24; plagioclase 8; clinopyroxene 6; epidote 26; amphibole 23; zoisite 26.

(a)	c — garnet — r				plagioclase	
	1	2	5	9		59
SiO ₂	38.44	38.38	38.72	38.82	SiO ₂	66.02
TiO ₂	.05	.20	.02	.00	CaO	1.92
Al ₂ O ₃	21.70	21.71	21.93	22.15	Al ₂ O ₃	21.16
FeO	24.58	24.78	25.40	24.41	Na ₂ O	11.07
MnO	1.27	1.44	.55	.63	K ₂ O	.07
MgO	4.15	3.93	5.20	5.18	tot	100.24
CaO	10.41	10.15	8.82	8.47	Si	2.89
tot	100.60	100.59	100.64	99.66	Ca	.09
Si	5.97	5.96	5.98	6.03	Al	1.09
Ti	.006	.02	.002	.00	Na	.94
Al	3.97	3.97	3.99	4.05	K	.003
Fe ²⁺	3.19	3.22	3.28	3.16	tot	5.01
Mn	.16	.18	.07	.08	An	8.7
Mg	.96	.91	1.19	1.19		
Ca	1.73	1.69	1.46	1.41		
tot	15.98	15.95	15.97	15.92		
X _{Mg}	.23	.22	.26	.27		
Alm	52	53	54	54		
Prp	15	15	19	20		
Sps	2	3	1	1		
Grs	28	27	24	24		

(b)	c — clinopyroxene — r				epidote	
	11	27	12	10		42
SiO ₂	54.37	55.38	55.93	56.27	SiO ₂	35.96
Al ₂ O ₃	9.27	9.70	10.78	10.97	Al ₂ O ₃	21.67
FeO _T	6.09	6.16	5.48	5.41	FeO	14.89
MgO	8.59	8.51	8.09	8.01	MgO	.73
CaO	14.47	14.42	13.29	13.12	CaO	21.80
Na ₂ O	5.96	6.25	7.14	7.05	Na ₂ O	.02
tot	98.75	100.42	100.71	100.83	tot	95.07
Si	1.98	1.97	1.98	1.98	Si	6.09
Al	.39	.41	.45	.45	Al	4.33
Fe ²⁺	.109	.108	.072	.104	Fe ²⁺	2.11
Fe ³⁺	.076	.075	.089	.055	Fe ³⁺	-
Mg	.46	.45	.42	.42	Mg	.18
Ca	.56	.55	.50	.49	Ca	3.96
Na	.41	.43	.48	.48	Na	.00
tot	3.98	3.99	3.99	3.97	tot	16.67
Jd	34	35	39	42		

(c)	amphibole				zoisite	
	41	22	51	60		28
SiO ₂	39.02	44.63	42.34	47.66	SiO ₂	38.94
TiO ₂	.32	.40	.49	.29	TiO ₂	.23
Al ₂ O ₃	19.27	12.52	15.31	11.37	Al ₂ O ₃	27.81
FeO	15.24	14.69	11.71	9.71	FeO	6.82
MnO	.16	.12	.11	.00	MnO	.06
MgO	8.28	11.34	10.79	14.21	MgO	.15
CaO	9.67	9.70	8.63	9.82	CaO	23.42
Na ₂ O	4.42	3.80	4.85	3.67	Na ₂ O	.03
K ₂ O	.28	.51	.49	.31	K ₂ O	.02
tot	96.66	97.71	94.72	97.04	tot	97.48
Si	5.82	6.52	6.35	6.84	Si	6.14
Al ^{IV}	2.17	1.47	1.65	1.15	Al	5.16
Al ^{VI}	1.21	.69	1.06	.77	Ti	.027
Ti	.036	.044	.055	.031	Fe	.89
Fe ²⁺	1.49	1.34	1.29	.96	Mn	.00
Fe ³⁺	.43	.45	.17	.20	Mg	.03
Mn	.02	.01	.01	.00	Ca	3.95
Mg	1.84	2.47	2.41	3.04	Na	.00
Ca	1.54	1.51	1.38	1.51	K	.00
Na ^{M4}	.45	.48	.61	.49	tot	16.19
Na ^A	.82	.59	.79	.53		
K	.05	.09	.09	.05		
■	.12	.30	.10	.41		
tot	15.99	15.96	15.96	15.99		
X _{Mg}	.55	.64	.65	.75		
Tr-Ed	4.34	2.38	3.90	1.61		
(Prg-Hs)						
-Tr	3.61	1.26	2.65	0.50		

ing pressures from 14 to 16 kbar during the eclogitic event.

A post-eclogitic decompression was recorded by the Ca-amphiboles. High Al^{VI} contents indicate pressures exceeding 5 kbar (Raase, 1974); high Na_{M4} in combination with high Al^{IV} suggests pressures of more than 7 kbar (Brown, 1977). Activities of amphiboles, coexisting with zoisite, albitic plagioclase and rutile, were calculated (Triboulet and Audren, 1985b; 1988) and the equilibria were applied tentatively to the empirical geothermobarometer of Triboulet (1992). Values from most amphiboles are beyond the calibration and only equilibria from late amphi-

boles (No. 60, Table 1) plot near the high-temperature limit of the isopleths at around 700 °C, 9 kbar, giving a further rough approximation of post-eclogitic P-T conditions. Amphiboles and clinopyroxenes both form a L>S fabric of a mineral lineation and a planar anisotropy. This implies that the high-pressure event as well as the overprinting by decompression proceeded during the fabric-producing deformation D₁-D₂.

Microstructures in mica schists

Kyanite-staurolite-garnet mica schists in a 50 m thick horizon, structurally 300 m below the

metabasites were sampled near Mirschachscharte (Fig. 1c). One sample (no. 2) with biotite, muscovite, quartz, garnet, plagioclase, staurolite, kyanite and ilmenite in typical microstructural positions, has been selected for microprobe analyses out of a dozen samples from the same horizon. The mode of plagioclase (plagioclase 5%, garnet 15%) in sample 2 is higher than in the other samples from the horizon, but lower than observed in other mica schists of the region (Troll and Hölzl, 1974; Troll *et al.*, 1976, 1980).

In XZ-sections parallel to the crenulation lineation, a planar or slightly anastomosing main foliation S_2 with biotite (Bt2), muscovite (Ms2) and kyanite surrounds microlithons with garnet, staurolite, kyanite, plagioclase (P12, P13), mica and quartz. Layers of pure quartz underline the foliation. Many muscovites have recrystallized with decussate orientation in the foliation planes, whereas biotite 2 in S_2 generally shows more distinct orientation. Large muscovites 3 overgrew the foliation planes (Fig. 3d). Garnets enclose biotite (Bt1), muscovite (Ms1), plagioclase (P11), quartz and ilmenite of an older foliation S_1 which sometimes lines up with the external S_2 (Fig. 3b, e). A slight postcrystalline rotation of some porphyroblasts is observed. Some garnets bear distinct inclusion-rich zones with numerous sub-microscopic needles (possibly zoisite?). The zones are oriented parallel to S_1 (Fig. 3b, e) or form concentric inner rims (Fig. 3f) in the porphyroblasts.

Early plagioclase (P11) is found in cores, in inclusion-rich zones and in rims of the garnets (Fig. 3a, b). Plagioclase 2 is situated between quartz grains in the microlithons (Fig. 3c) and plagioclase 3 forms porphyroblasts with inclusions of small muscovite (Fig. 3d, e). Sometimes, plagioclase 2 and 3 are in contact with garnet rims (Fig. 3c). Optically zoned staurolite with inclusion-free large cores and quartz-inclusion-rich small rims appears with kyanite near to garnet rims (Fig. 3a) and outside the microlithons. Some of the staurolites enclose garnet, while others are mantled by small kyanite.

The successive mineral assemblages can be derived directly from the successive appearance of phases (Fig. 4) in a microstructural-mineralogical scheme (Triboulet and Audren 1985a). This scheme is based on the relative temporal appearance of the phases in relation to successive foliations S_1 and S_2 which were generated in the mica schists by progressive deformation D_1 – D_2 . Assemblage M_1 of an early stage of metamorphism consists of biotite, muscovite, plagioclase and garnet. Kyanite inside the microlithons probably accompanies this assemblage. A sub-

sequent assemblage M_2 is: biotite, muscovite, garnet, plagioclase, kyanite and staurolite (Fig. 4). The microstructures suggest that growth of garnet stopped after the appearance of staurolite. Evidently, assemblages M_1 and M_2 grew during the formation of the main foliation S_2 . The crystallization of staurolite and kyanite continued after generation of S_2 (Troll *et al.*, 1976; Behrmann, 1990). Growth of large muscovites 3 as well as recrystallization of muscovites postdate the foliation-forming shearing.

Mineral chemistry in a mica schist (sample 2)

Garnets show continuous growth zonations with variable almandine (Alm), spessartine (Sps), grossular (Grs) and pyrope (Prp) components (Fig. 5a, b). Spessartine contents in the cores (7%) are higher than in the rims (<2%) of the porphyroblasts, and the zones with abundant inclusions of needles are always correlated with constant high pyrope and grossular contents. This indicates a temporal evolution of garnet composition before and after to the formation of these zones. The evolution displays decreasing, then increasing grossular contents (from 6% to 2%, then to 7%) and increasing pyrope contents (from 10% to 17%) towards the inner part of the inclusion zones. Outside the zones, grossular contents then decrease (to 1%) while the pyrope component further increases up to 20% (Fig. 5c).

Early biotite (Bt1) enclosed by garnet has slightly higher X_{Mg} (0.57–0.56) compared with biotite forming the main foliation S_2 (X_{Mg} 0.55–0.54). Al^{VI} contents in biotite 1 are 2.45–2.53, and 2.48–2.73 in biotite 2. In biotite 1, Al^{VI} is 0.98–0.84, and in biotite 2 from 0.93 to 0.82. The range of Ti contents (0.18–0.21) is similar in both biotite generations, but most of the biotites 1 show lower Ti (0.18) than the second generation (Ti 0.20). Muscovites from different microstructural positions show different compositions. The early muscovite 1 inside garnets are Na-rich (0.3–0.4) and Si^{4+} -poor (6.2). Rare small muscovites 2 in quartz-rich layers have similar compositions. Fe and Mg contents of these muscovites 1 and 2 are $Fe = 0.05$ – 0.14 and $Mg = 0.09$ – 0.14 . Recrystallized muscovites in the foliation S_2 as well as late large muscovite 3 on the other hand display Na-poorer (0.2) and Si^{4+} -richer (6.4) compositions (Fig. 5d) with $Fe = 0.14$ – 0.16 and $Mg = 0.14$ – 0.43 . This implies a recrystallization of muscovites at lower temperatures (Cipriani *et al.*, 1971) after the final increment of deformation D_1 – D_2 . Staurolite porphyroblasts have X_{Mg}

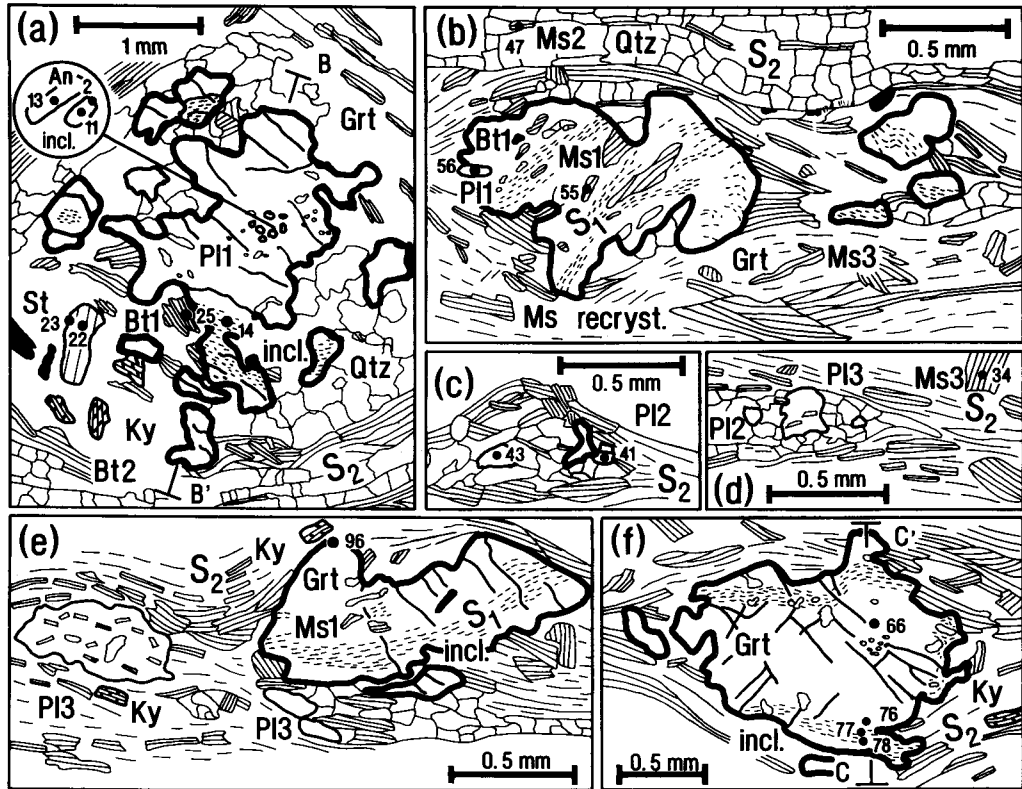


Fig. 3. Microstructures in kyanite-staurolite-garnet mica schist (sample 2) in XZ-sections parallel to the crenulation lincation. Numbers label analyses in Table 2 and Figs. 5 and 6. (a) Garnet enclosing unzoned and zoned albite plagioclase 1. Numbers in the inset to the left are anorthite contents in mole %. The garnet shows an inclusion-rich zone (incl.) near to the rim. See Fig. 5a for zoning profile. Staurolite and kyanite accompany the garnet near to its rim. (b) Garnet encloses foliation S_1 by muscovite 1, biotite 1, albite plagioclase and inclusion-rich zones. Decussate muscovites recrystallized (Ms recryst.) in S_2 . (c) Microlithon with garnet and interstitial twinned albite plagioclase 2 in contact. (d) Microlithon with interstitial plagioclase 2 and albite plagioclase 3. Large muscovite 3 crosscuts S_2 . (e) Microlithon with garnet and plagioclase 3 is surrounded by S_2 . S_1 by inclusions in garnet lines up with S_2 . (f) Garnet of zonation profile C-C' (Fig. 5b). Inclusion-rich zones are situated near to the rim.

from 0.20 to 0.24 with slightly higher Mn contents in the cores (Table 2c).

Some of the early plagioclases 1 in the spessartine-rich core of a large garnet (Fig. 3a) show optical and chemical zonation with An 11-13 in the core and An 2 in the rims. Other plagioclases (An 1-2) in the garnet cores are unzoned. The plagioclases 1 in inclusion-rich zones and in the pyrope-rich rims of garnets (Fig. 3b) are albitic as well. Similar albitic-rich compositions were observed from small plagioclase 2 and plagioclase 3 inside the microlithons. No plagioclase with anorthite contents exceeding 13%, as has frequently been observed from other mica schist horizons of the region (Troll *et al.*, 1976; 1980; Behrmann, 1990), was found in the investigated sample.

P-T estimates from a mica schist (sample 2)

The increasing X_{Mg} of zoned garnets are characteristic of a metamorphism prograde in temperature (Martignole and Nantel, 1982). Assemblage M_1 appears in a divariant field which is bounded by a garnet-forming reaction at low temperatures and a staurolite-producing reaction (Spear and Cheney, 1989) at high temperatures. Assemblage M_2 with staurolite seems to appear at increasing temperature and decreasing pressure by continuous reactions garnet + chlorite + muscovite = staurolite + biotite + H_2O , or garnet + biotite + Al_2SiO_5 + H_2O = staurolite + muscovite + quartz (Spear and Cheney, 1989), as is indicated by decreasing X_{Ca} and increasing X_{Mg} in garnet rims and further increasing X_{Mg} in

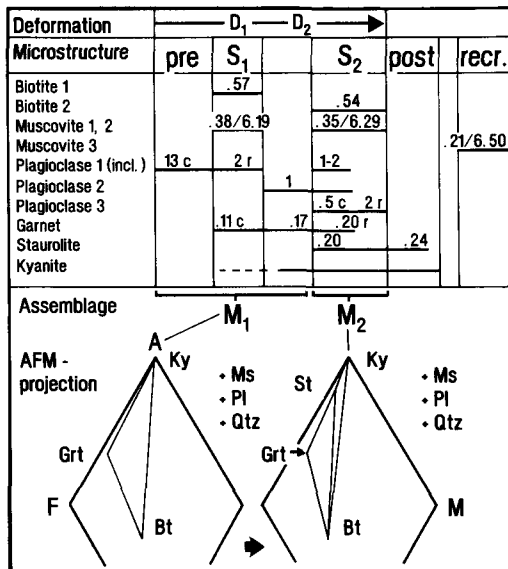


FIG. 4. Mineralogical-microstructural scheme from the mica schist (sample 2). Successive appearance of phases in relationship to microstructures of deformation D₁-D₂, and successive assemblages M₁ and M₂ in AFM-projections. Numbers in the diagram refer to mineral chemistry of biotite (X_{Mg}), muscovite (Na/Si⁴⁺), plagioclase (An mole %), garnet (X_{Mg}) and staurolite (X_{Mg}); c core, r rim.

staurolite. Garnet growth then seems to have stopped after the appearance of staurolite (Fig. 4). Changes in garnet composition can be explained by continuous reactions among garnet, biotite, muscovite and plagioclase inside the divariant field, depending on P and T (Thompson, 1976; Trzcieski, 1977; Tracy, 1982). It is possible to use the garnet zonation trend within low-variance assemblages to derive $\Delta T/\Delta P$ trends by the Gibbs method (Spear and Selverstone, 1983; Spear *et al.*, 1984; Haugerud and Zen, 1991). Each step of garnet chemical evolution represents a finite temporal and spatial domain of equilibration with the other minerals of the assemblage. Thus, when coexistent minerals are preserved as inclusions or within the microstructural domain of interest ('local equilibrium'), and when their chemical compositions are known, P and T can be evaluated by 'classical' thermobarometry (Perchuk *et al.*, 1985; Triboulet and Audren, 1985a; St-Onge, 1987; Haugerud and Zen, 1991).

However, each generation of mica seems to have been homogenized after a finite time interval of deformation (Triboulet and Audren, 1985a). Despite a strong increase of X_{Mg} in

garnets, biotites show only a slight change towards lower X_{Mg} in the younger foliation S₂ and it is probable that garnet coexisted with biotites of X_{Mg} 0.57 to 0.54 throughout its growth (Fig. 4). Only muscovite 1 and 2 with Na-rich and Si-poor compositions are considered to have coexisted with the other M₁ and M₂ phases. Recrystallized decussate muscovites in S₂ and muscovite 3 with Na-poor and Si-rich compositions grew after the M₁-M₂ metamorphism (Fig. 4).

Although garnet shows significant Ca variation, the anorthite contents of coexisting plagioclases (enclosed or in the matrix) change only slightly within an albite-rich range. Slow rates of post-entrapment volume diffusion in plagioclases will preserve original compositions of inclusions inside garnets (St-Onge, 1987). The only effective means of equilibration is for old plagioclase to dissolve partially or completely, and for new plagioclase of a different composition to grow (Spear *et al.*, 1990). No textural signs of a retrograde albitisation of initially anorthite-richer plagioclase and of coexisting oligoclase and albite (Ashworth and Evirgen, 1985a) were found. Thus, formation of the zoned enclosed plagioclase (An 13% to An 2% from core to rim) probably predated the garnet growth. Garnet growth started with the crystallization of albitic plagioclase. Furthermore, albitic plagioclase appears in Ca- and Mg-rich inclusion-bearing zones, in Mg-rich rims of garnet, in close contact with the garnets and outside them within the microlithons. Following these microstructural observations, garnet is considered to have grown and coexisted with albitic plagioclases throughout the M₁-M₂ metamorphism. Oligoclase and andesine as well as anorthite-rich rims around anorthite-poor cores observed in Ca-richer other mica schists of the region (Troll *et al.*, 1976; 1980; Behrmann, 1990) are possibly related to a post-M₁-M₂ stage of metamorphism.

Temperatures from the garnet-bearing assemblage were calculated by applying five garnet-biotite Fe-Mg exchange geothermometers (Thompson, 1976; Holdaway and Lee, 1977; Hodges and Spear, 1982; Ganguly and Saxena, 1984; Perchuk and Aranovitch, 1984) to typical analyses from the garnet zonation trend (Fig. 5c). Analyses of biotite 1 (No. 25, Table 2b) and an early step of garnet evolution (No. 66, 76, 77, Table 2a) were combined. Biotite 2 (No. 84) was related to a late step of garnet zonation (No. 14, 78, 96). The pressure variation was estimated by applying the garnet analyses to four garnet-plagioclase Ca-net-transfer geobarometers involving aluminosilicate (Newton and Haselton, 1981; Ganguly and Saxena, 1984; Perchuk *et al.*,

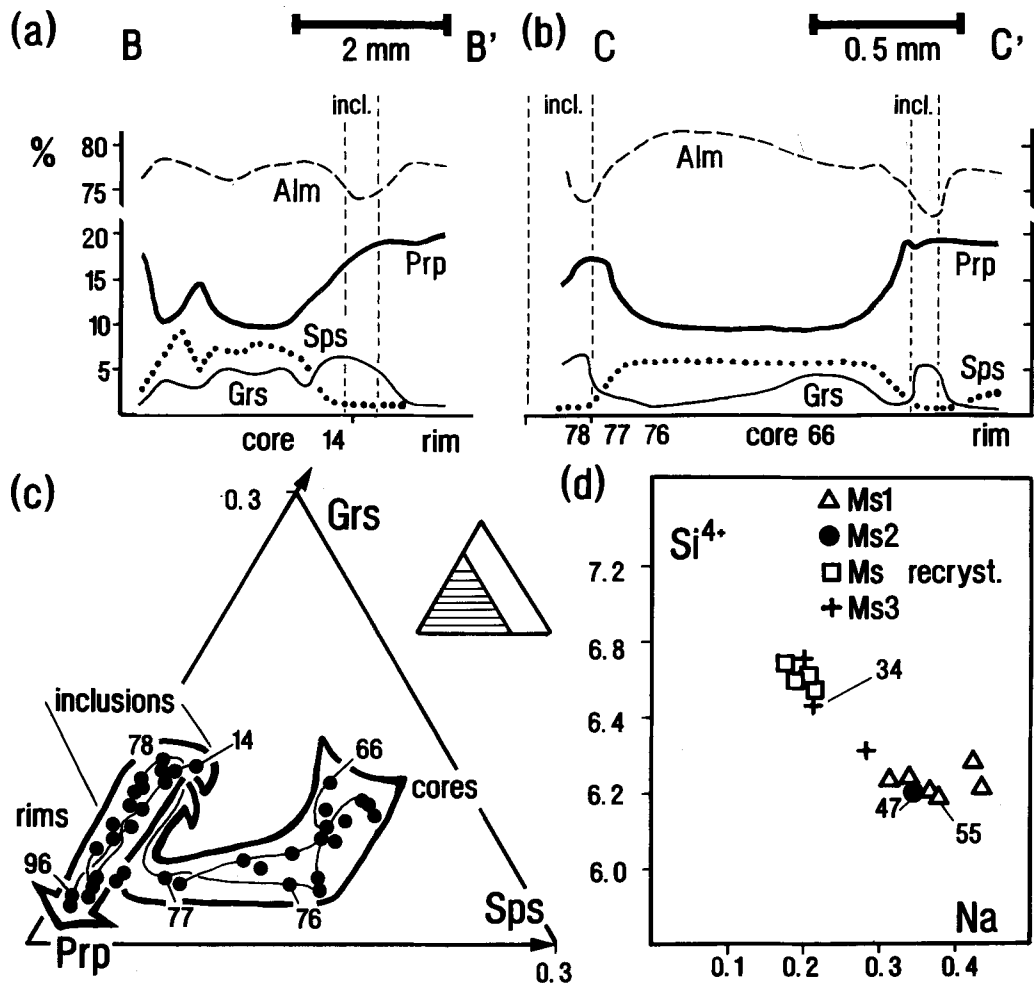


Fig. 5. Mineral chemistry in kyanite-staurolite-garnet mica schist (sample 2). Numbers refer to analyses in Figs. 3 and 6. (a) Zonation profile of garnet in Fig. 3a. The positions of inclusion-rich zones (incl.) are marked. (b) Zonation profile of the garnet in Fig. 3f. (c) Evolution of garnet compositions in grossular (Grs)-pyrope (Prp)-spessartine (Sps) coordinates. Large arrows indicate the chemical trend. Numbers refer to selected analyses in Fig. 6. (d) Chemical compositions of the muscovites in Si^{4+} versus Na diagram.

1985; Koziol and Newton, 1988). Due to the possibly questionable presence of kyanite in the assemblage throughout garnet growth, the calibration of Ghent and Stout (1981) which is applicable to assemblages lacking aluminosilicates has been used additionally. Garnet analyses (66, 76, 77, 14, 78, 96) were combined with an unzoned plagioclase (No. 3 with An 2%) from a garnet inclusion, and with syn- S_1 muscovite 1 (No. 55) respectively. This is possible because garnet was found to have coexisted with albitic plagioclase throughout its growth (see above). Due to the low anorthite contents in the other plagioclases, results from calculations involving

other enclosed plagioclases in garnets cores and rims, plagioclase in contact with garnet rims, and plagioclase in the microlithons, only differ slightly (<1.5 kbar) from the P estimates yielded by the method described above.

Poorly understood activity/composition relationships in plagioclase An <20% at low T (Ashworth and Evirgen, 1985a, b) and a possible strong positive deviation from ideality for plagioclase An <5-8% (Ghent and Stout, 1981) suggest that pressure estimates from garnet and albitic plagioclase may be doubtful and too high. Compared with the results for the eclogitic stage in the metabasite (14-16 kbar at 550-650°C, Fig. 6b),

TABLE 2. (a)–(c) Microprobe analyses from kyanite–staurolite–garnet mica schist (sample 2), selected from 110 analyses. Numbers of oxygens: garnet 24; biotite (Bt) 22; muscovite (Ms) 22; plagioclase (Pl) 8; staurolite 23.5. c = cores, r = rims of minerals, re = recrystallized.

(a)	garnet					
	c 66	76	77	14	78	r 96
SiO ₂	36.70	36.51	37.21	37.06	36.96	37.32
TiO ₂	.02	.02	.00	.06	.10	.00
Al ₂ O ₃	20.73	20.95	21.04	21.17	20.93	21.23
FeO	34.79	35.26	34.99	35.01	33.54	34.81
MnO	2.44	2.61	1.32	.77	.44	.20
MgO	2.48	3.12	4.33	3.68	4.47	5.09
CaO	1.87	.68	.83	2.20	2.61	.66
tot	99.03	99.15	99.72	99.95	99.05	99.31
Si	5.99	5.95	5.97	5.95	5.95	5.97
Ti	.001	.002	.00	.007	.011	.00
Al	3.98	4.02	3.98	4.00	3.97	4.00
Fe ²⁺	4.75	4.80	4.69	4.70	4.51	4.66
Mn	.33	.36	.18	.10	.06	.02
Mg	.60	.75	1.03	.88	1.07	1.21
Ca	.32	.11	.14	.37	.45	.11
tot	15.97	15.99	15.99	16.00	16.02	15.96
X _{Mg}	.11	.13	.18	.15	.19	.20
Alm	78	79	77	77	74	77
Prp	10	12	17	14	17	20
Sps	5	5	2	1	.98	.44
Grs	5	1.8	2.2	6	7	1.7

(b)	micas					
	Bt1	Bt2	Ms1	Ms2	Ms2re	Ms3
	25	84	55	47	85	34
SiO ₂	37.49	36.57	48.21	49.83	52.78	49.85
TiO ₂	1.71	1.84	.47	.48	.67	.81
Al ₂ O ₃	20.14	19.25	37.52	38.06	33.37	32.39
FeO	16.28	17.30	1.37	.51	1.34	1.48
MgO	12.25	11.69	.76	.53	2.13	2.26
Na ₂ O	.36	.24	1.55	1.43	.79	.85
K ₂ O	6.99	8.28	6.27	6.04	6.53	7.54
tot	95.22	95.17	96.15	96.88	97.61	95.18
Si	5.50	5.45	6.19	6.29	6.64	6.50
Ti	.18	.20	.04	.04	.06	.07
Al	3.48	3.38	5.67	5.66	4.94	4.98
Fe ²⁺	1.99	2.16	.14	.05	.14	.16
Mg	2.67	2.60	.14	.09	.40	.43
Na	.10	.06	.38	.35	.19	.21
K	1.30	1.57	1.02	.97	1.04	1.25
tot	15.22	15.42	13.58	13.45	13.41	13.60
X _{Mg}	.57	.54				

(c)	plagioclase				staurolite
	Pl1c	Pl1r	Pl2	Pl3	23
	100	3	41	43	
SiO ₂	65.90	68.50	70.05	69.49	SiO ₂ 28.16
CaO	2.59	.45	.18	.07	TiO ₂ .45
Na ₂ O	9.47	10.72	9.58	10.58	Al ₂ O ₃ 52.28
K ₂ O	.08	.07	.02	.06	FeO 11.96
Al ₂ O ₃	22.40	20.67	20.40	20.05	MgO 2.19
tot	100.44	100.41	100.23	100.25	tot 95.04
Si	2.86	2.96	3.01	3.00	Si 3.98
Ca	.12	.02	.008	.003	Ti .04
Na	.79	.90	.79	.88	Al 8.71
K	.004	.004	.001	.003	Fe 1.41
Al	1.14	1.05	1.03	1.02	Mg .46
tot	4.91	4.93	4.83	4.90	tot 14.60
An	13.05	2.24	1.03	.38	X _{Mg} .24

corresponding pressure estimates from garnet–plagioclase–aluminosilicate–quartz barometers are considerably higher (18 and 19.5 kbar at 650 °C, Fig. 6a), whereas results from Ghent and Stout (1981) (14.5 kbar at 650 °C, Fig. 6a) are lower. Consequently, minimal and maximal results from all applied geothermobarometers define successive *P–T* fields encompassing the disagreements among all the calibrations, but giving evidence that both mica schists and eclogitic amphibolites suffered similar high-pressure metamorphism (Fig. 6b). The *P–T* fields line up and form a syn-*D*₁–*D*₂ *P–T* path with a characteristic shape. All the geothermobarometers for metapelites involve the garnet activity model as a predominant part, and micas and plagioclases as a

minor part of calculations. Thus, when calculated from characteristic analyses of the garnet zonation trend, the results will always give a *P–T* path strongly dependant on the easily-measurable chemical zonation of the garnet. Due to the slight compositional variations of coexisting micas and plagioclases, this effect is intensified. On the one hand, the *P–T* path mainly follows the garnet Ca and Mg zonation trend and gives a relative *P–T* evolution as from garnet zonation modelling. On the other hand, this path is defined by actual *P–T* estimates from garnets and continuously coexisting micas and albitic plagioclase.

The *P–T* path from sample 2 describes decreasing–increasing pressures at increasing temperatures (460 °C, 11 kbar to 480 °C, 7.5 kbar and then

deformative and must also be post-Upper-Ordovician.

Compared with the results from the eclogitic amphibolites, pressures calculated from garnet and albitic plagioclase (An 2%) in mica schists are overestimated by Grt-Pl-As-Qtz geobarometers and underestimated by the Grt-Bt-Ms-Pl calibration. Mean values from geothermobarometry in mica schists give similar high pressures at equivalent temperatures as the estimates from metabasites and confirm that garnet-plagioclase Ca-net-transfer barometers work in the relevant P - T field. The crystallization of late-S₂ and post-S₂ amphibolite-facies assemblages postdated the high-pressure metamorphism and occurred during a decompression section of the same P - T path. A final decompression path for the lower part of the lithotectonic unit can be inferred by assuming mainly erosional uplift (England and Thompson, 1984) and reached P - T conditions of anatectic melting (Hoke, 1990) in the adjacent Kreuzeckgruppe (Fig. 6b).

At first glance, the mica cooling ages around 70–90 Ma in the region (Oxburgh *et al.*, 1966; Brewer, 1969; Troll, 1978) indicate an early-Alpine minimum age of this metamorphism. However, it must be taken into account that the pre-Alpine basement suffered an early-Alpine overprinting. This is obvious from late-Variscan mica cooling ages around 260–300 Ma in the southern parts of the basement (Brewer, 1969; Borsi *et al.*, 1978; Sassi *et al.*, 1985; Hoke, 1990) and from successively younger Variscan–Alpine ‘mixing ages’ to the north (Hoke, 1990). Thus, a pre-Alpine and post-Upper-Ordovician age of the high-pressure metamorphism in the Schobergruppe appears to be possible too. As it has been outlined above, garnet compositional zonation reflects a history of continuous reactions depending on P and T of metamorphism. Consequently, garnet zonation trends and the derived P - T evolutions are characteristic properties of a geological unit. Similar garnet zonation trends to those in the Schobergruppe were recognized from mica schists of the same lithotectonic unit in the Deferegger Alps, 30 km to the west (Figs. 1b, 6a inset). P - T paths from these mica schists (Schulz, 1990) display a similar marked decompression-compression (Fig. 6b). In this part of the basement, exclusively late-Variscan Rb–Sr mica ages were found (Borsi *et al.*, 1978; Sassi *et al.*, 1985) which date the cooling after the amphibolite-facies stage of metamorphism (Stöckhert, 1985; Schulz, 1990). Hence, this similarity of garnet zonation trends and P - T path shapes in the Deferegger Alps and Schobergruppe points to an early-Variscan age of high-pressure and sub-

sequent amphibolite-facies metamorphism in the Prijakt area. In the Schobergruppe, late-Variscan cooling ages are lacking. Early-Alpine thermal overprinting probably extinguished the Variscan radiometric traces. The recrystallization of muscovites and the crystallization of new muscovite 3 in the mica schists at temperatures below 500 °C presumably can be related to the partial early-Alpine rejuvenation of this part of the Austroalpine basement.

Acknowledgements

C. Triboulet, CNRS Paris, and C. Audren, CNRS Rennes, provided unpublished data, facilitated research stays of the author at Paris and Rennes, and checked the manuscript. Microprobe analyses at Mineralogisches und Petrologisches Institut der Universität Bonn were assisted by B. Spiering and M. Schumacher. A thorough and constructive review by J. R. Ashworth (Birmingham) improved the manuscript. The work was financed by a research grant (Schu 676-1) from the Deutsche Forschungsgemeinschaft.

References

- Ashworth, J. R. and Evirgen, M. M. (1985a) Plagioclase relations in pelites, central Menderes Massif, Turkey. I. The peristerite gap with coexisting kyanite. *J. Metamorphic Geol.*, **3**, 207–18.
- (1985b) Plagioclase relations in pelites, central Menderes Massif, Turkey. II. Perturbation of garnet-plagioclase geobarometers. *Ibid.*, **3**, 219–30.
- Becker, L. P., Frank, W., Höck, V., Kleinschmidt, G., Neubauer, F., Sassi, F. P., and Schramm, J. M. (1987) Outlines of pre-Alpine events in the Austrian Alps. In *Pre-Variscan and Variscan events in the Alpine-Mediterranean mountain belts* (Flügel, H. W., Sassi, F. P., and Grecula, P., eds.), 69–106. Alfa Publishers, Bratislava.
- Behrmann, J. H. (1990) Zur Kinematik der Kontinentkollision in den Ostalpen. *Geotekt. Forsch.*, **76**, 1–180.
- Borsi, S., Del Moro, A., Sassi, F. P., and Zirpoli, G. (1973) Metamorphic evolution of the Austridic rocks to the south of the Tauern Window (Eastern Alps): radiometric and geopetrologic data. *Mem. Soc. Geol. Ital.*, **12**, 549–71.
- Zanferrari, A., and Zirpoli, G. (1978) New geopetrologic and radiometric data on the Alpine history of the Austridic continental margin south of the Tauern Window. *Mem. Ist. Geol. Min. Univ. Padova*, **32**, 1–19.
- Brewer, M. S. (1969) Excess radiogenic argon in metamorphic micas from the Eastern Alps, Austria. *Earth Planet. Sci. Lett.*, **6**, 321–31.
- Brown, E. H. (1977) The crossite content of Ca-amphibole as a guide to pressure of metamorphism. *J. Petrol.*, **18**, 53–72.
- Cipriani, C., Sassi, F. P. and Scolari, A. (1971)

- Metamorphic white micas: definition of paragenetic fields. *Schweiz. Mineral. Petrogr. Mitt.*, **51**, 259–302.
- Clar, E. (1927) Ein Beitrag zur Geologie der Schobergruppe bei Lienz in Tirol. *Mitt. Naturwiss. Ver. Steiermark*, **63**, 72–90.
- Cliff, R. A. (1980) U–Pb isotopic evidence from zircons for lower Palaeozoic tectonic activity in the Austroalpine nappe, the Eastern Alps. *Contrib. Mineral. Petrol.*, **71**, 283–8.
- Ebner, F., Neubauer, F. and Statterger, K. (1987) The Caledonian event in the Eastern Alps: A review. In *Pre-Variscan and Variscan events in the Alpine-Mediterranean mountain belts* (Flügel, H. W., Sassi, F. P., and Grecula, P., eds.), 169–82. Alfa Publishers, Bratislava.
- Ellis, D. J. and Green, D. H. (1979) An experimental study of the effect of Ca upon garnet–clinopyroxene Fe–Mg exchange equilibria. *Contrib. Mineral. Petrol.*, **71**, 13–22.
- England, P. C. and Thompson, A. B. (1984) Pressure–temperature–time paths of regional metamorphism. I. Heat transfer during the evolution of regions of thickened continental crust. *J. Petrol.*, **25**, 894–928.
- Ganguly, J. and Saxena, S. K. (1984) Mixing properties of aluminosilicate garnets: constraints from natural and experimental data, and applications to geothermobarometry. *Am. Mineral.*, **69**, 88–97.
- Gasparik, T. and Lindsley, D. H. (1980) Phase equilibria at high pressure of pyroxenes containing monovalent and trivalent ions. In *Pyroxenes* (Prewitt, C. T., ed.) *Reviews in Mineralogy*, **7**, Min. Soc. Am., 309–36.
- Ghent, E. D. and Stout, M. Z. (1981) Geobarometry and geothermometry of plagioclase–biotite–garnet–muscovite assemblages. *Contrib. Mineral. Petrol.*, **76**, 92–7.
- Hammerschmidt, K. (1981) Isotopengeologische Untersuchungen am Augengneis vom Typ Campo Tures bei Rain in Taufers, Südtirol. *Mem. Ist. Geol. Min. Univ. Padova*, **34**, 273–300.
- Haugerud, R. A. and Zen, E. A. (1991) An essay on metamorphic path studies or Cassandra in P – T – τ space. In *Progress in metamorphic and magmatic petrology* (Perchuk, L. L., ed.), 323–48. Cambridge University Press.
- Hodges, K. V. and Spear, F. S. (1982) Geothermometry, geobarometry and the Al_2SiO_5 triple point at Mt. Moosilauke, New Hampshire. *Am. Mineral.*, **67**, 1118–34.
- Hoinkes, G., Purtscheller, F., and Tessadri, R. (1982) Polymetamorphose im Ostalpin westlich der Tauern (Ötztaler Masse, Schneeberger Zug, Brennermesozoikum). *Geol. Paläont. Mitt. Innsbruck*, **12**, 95–113.
- Kostner, A., and Thöni, M. (1991) Petrologic constraints for Eoalpine eclogite facies metamorphism in the Austroalpine Ötztal basement. *Mineralogy and Petrology*, **43**, 237–54.
- Hoke, L. (1990) The Altkristallin of the Kreuzeck Mountains, SE Tauern Window, Eastern Alps—basement crust in a convergent plate boundary zone. *Jb. Geol. B.-A.*, **133**, 5–87.
- Holdaway, M. J. and Lee, S. M. (1977) Fe–Mg cordierite stability in high-grade pelitic rocks based on experimental, theoretical and natural observations. *Contrib. Mineral. Petrol.*, **63**, 175–98.
- Holland, T. J. B. (1983) The experimental determination of activities in disordered and short-range ordered jadeitic pyroxenes. *Ibid.*, **82**, 214–20.
- Kozioł, A. M. and Newton, R. C. (1988) Redetermination of the anorthite breakdown reaction and improvement of the plagioclase–garnet– Al_2SiO_5 –quartz geobarometer. *Am. Mineral.*, **73**, 216–23.
- Krogh, E. J. (1988) The garnet–clinopyroxene Fe–Mg geothermometer—a reinterpretation of existing experimental data. *Contrib. Mineral. Petrol.*, **99**, 44–8.
- Leake, B. A. (1978) Nomenclature of amphiboles. *Am. Mineral.*, **63**, 1023–52.
- Maggetti, M. and Galetti, G. (1988) Evolution of Silvretta eclogites: metamorphic and magmatic events. *Schweiz. Mineral. Petrogr. Mitt.*, **68**, 467–84.
- Manby, G. M. and Thiedig, F. (1988) Petrology of eclogites from the Saualpe (Austria). *Ibid.*, **68**, 441–66.
- Martignole, J. and Nantel, S. (1982) Geothermobarometry of cordierite-bearing metapelites near the Morin anorthosite complex, Grenville province, Quebec. *Canad. Mineral.*, **20**, 307–18.
- Massonne, H.-J. and Schreyer, W. (1987) Phengite geobarometry based on the limiting assemblage with K-feldspar, phlogopite and quartz. *Contrib. Mineral. Petrol.*, **96**, 212–24.
- Miller, C. (1990) Petrology of the type locality eclogites from the Koralpe and Saualpe (Eastern Alps), Austria. *Schweiz. Mineral. Petrogr. Mitt.*, **70**, 287–300.
- Mogessie, A. and Purtscheller, F. (1986) Polymetamorphism of the Oetztal-Stubai basement complex based on amphibolite petrology. *Jb. Geol. B.-A.*, **129**, 69–91.
- Newton, R. C. and Haselton, H. T. (1981) Thermodynamics of the garnet–plagioclase– Al_2SiO_5 –quartz geobarometer. In *Thermodynamics of minerals and melts* (Newton, R. C., Navrotsky, A., and Wood, B. J., eds.), 131–47. Springer Verlag, New York.
- Oxburgh, E. R., Lambert, R. S., Baadsgard, H. and Simons, J. G. (1966) Potassium–argon age studies across the southeast margin of the Tauern Window in the Eastern Alps. *Verh. Geol. B.-A.*, 17–33.
- Papike, J. J. (1974) On the chemistry of clinopyroxenes. *EOS Trans. Geophys. Union*, **55/4**, 469.
- Perchuk, L. L. and Aranovitch, L. Y. (1984) Improvement of garnet–biotite geothermometer: correction for fluorine content in biotite. *Dokl. Acad. Sci. USSR*, **277**, 471–5, (in Russian).
- Podlesskii, K. K., Lavrant'eva I. V., Gerasimov, V. Y., Fed'kin, V. V., Kitsul, V. I., Karsakov, L. P. and Berdnikov, N. V. (1985) Precambrian granulites of the Aldan shield, eastern Siberia, USSR. *J. Metamorphic Geol.*, **3**, 265–310.
- Perkins, D. and Newton, R. C. (1981) Charnockitic geobarometers based on coexisting garnet–pyroxene–plagioclase–quartz. *Nature*, **292/9**, 144–46.
- Raase, P. (1974) Al and Ti contents of hornblende indicators of pressure and temperature of regional metamorphism. *Contrib. Mineral. Petrol.*, **45**, 231–6.

- Raheim, A. and Green, D. H. (1974) Experimental determination of the temperature and pressure dependence of the Fe–Mg partition coefficient for coexisting garnet and clinopyroxene. *Ibid.*, **48**, 179–203.
- Richter, W. (1973) Vergleichende Untersuchungen an ostalpinen Eklogiten. *Tschermaks Mineral. Petrogr. Mitt.*, **19**, 1–34.
- Sassi, F. P., Cavazzini, G., Visoná, D. and Del Moro, A. (1985) Radiometric geochronology in the Eastern Alps: results and problems. *Rend. Soc. Ital. Mineral. Petr.*, **40**, 187–224.
- Schulz, B. (1990) Prograde–retrograde P – T – t deformation path of Austroalpine micaschists during Variscan continental collision (Eastern Alps). *J. Metamorphic Geol.*, **8**, 629–43.
- Nollau, G., Heinisch, H. and Godizart, G. (1993) Austroalpine basement complex to the south of the Tauern Window. In *The pre-Mesozoic geology of the Alps* (von Raumer, J. F. and Neubauer, F., eds.), 493–512. Springer Verlag Heidelberg.
- Spear, F. S. and Cheney, J. T. (1989) A petrogenetic grid for pelitic schists in the system SiO_2 – Al_2O_3 – FeO – MgO – K_2O – H_2O . *Contrib. Mineral. Petrol.*, **101**, 149–64.
- and Rumble, D. (1986) Pressure, temperature and structural evolution of the Orfordville Belt, West-Central New Hampshire. *J. Petrol.*, **27**, 1071–93.
- and Selverstone, J. (1983) Quantitative P – T paths from zoned minerals: theory and tectonic applications. *Contrib. Mineral. Petrol.*, **83**, 348–57.
- Hickmott, D., Crowley, P. and Hodges, K. V. (1984) P – T paths from garnet zoning: a new technique for deciphering tectonic processes in crystalline terranes. *Geology*, **12**, 87–90.
- Kohn, M. J., Florence, F. P. and Menard, T. (1990) A model for garnet and plagioclase growth in pelitic schists: implications for thermobarometry and P – T path determinations. *J. Metamorphic Geol.*, **8**, 683–96.
- Stöckhert, B. (1985) Pre-Alpine history of the Austridic basement to the south of the western Tauern Window (Southern Tyrol, Italy)—Caledonian versus Hercynian event. *Neues Jahrb. Geol. Paläont. Mh.*, 618–42.
- St-Onge, M. R. (1987) Zoned poikiloblastic garnets: P – T paths and syn-metamorphic uplift through 30 km of structural depth, Wopmay orogen, Canada. *J. Petrol.*, **28**, 1–21.
- Thompson, A. B. (1976) Mineral reactions in pelitic rocks. *Am. J. Sci.*, **276**, 401–54.
- Tracy, R. J. (1982) Compositional zoning and inclusions in metamorphic minerals. In *Characterization of metamorphism through mineral equilibria* (Ferry, J. M., ed.), *Reviews in Mineralogy*, **10**, Min. Soc. Am., 355–97.
- Triboulet, C. (1992) The (Ca–Na) amphibole–albite–chlorite–epidote–quartz geothermobarometer in the system S – A – F – M – C – N – H_2O . 1. An empirical calibration. *J. Metamorphic Geol.*, **10**, 545–56.
- and Audren, C. (1985a) Continuous reactions between biotite, garnet, staurolite, kyanite/sillimanite/andalusite and P – T –time deformation path in the micaschists from the estuary of the River Vilaine, South Brittany, France. *Ibid.*, **3**, 91–105.
- (1985b) Evolution des amphiboles et leurs associations au cours d'un métamorphisme progressif polyphasé. Exemple d'une métabasite de la Vilaine. *Schweiz. Mineral. Petrogr. Mitt.*, **65**, 279–98.
- (1988) Controls on P – T – t deformation path from amphibole zonation during progressive metamorphism of basic rocks (estuary of the River Vilaine, South Brittany, France). *J. Metamorphic Geol.*, **6**, 117–33.
- Troll, G. (1978) The 'Altkristallin' of Eastern Tyrol between Tauern Window and Periadriatic Lineament. In *Alps, Apennines, Hellenides* (Closs, H., Roeder, D. and Schmidt, K., eds.), Inter-Union Commission on Geodynamics Scientific Report No. 38, 149–54. Schweizerbart, Stuttgart.
- and Hölzl, E. (1974) Zum Gesteinsaufbau des Altkristallins der zentralen Schobergruppe, Osttirol. *Jb. Geol. B.-A.*, **117**, 1–16.
- Forest, R., Söllner, F., Brack, W., Köhler, H., and Müller-Sohnius, D. (1976) Über Bau, Alter und Metamorphose des Altkristallins der Schobergruppe, Osttirol. *Geol. Rdsch.*, **65**, 483–511.
- Baumgartner, S., and Daiminger, W. (1980) Zur Geologie der südwestlichen Schobergruppe (Osttirol, Österreich). *Mitt. Ges. Geol. Bergbaustud. Österr.*, **26**, 277–95.
- Trzcieski, W. E. (1977) Garnet zoning—product of a continuous reaction. *Canad. Mineral.*, **15**, 250–56.
- Velde, B. (1967) Si^{4+} contents of natural phengites. *Contrib. Mineral. Petrol.*, **14**, 250–8.

[Manuscript received 23 April 1992;
revised 13 July 1992]